ARTICLES

Theoretical study on Cl L_{23} NEXAFS and UV absorption data for metal chlorides

X. Qian, H. Sambe, and D. E. Ramaker
Department of Chemistry, George Washington University, Washington, D.C. 20052
(Received 22 May 1995)

An effective iterative decomposition procedure for separating the L_{23} NEXAFS line shape into the L_2 and L_3 components for the alkali halides has been developed. This decomposition allows a direct comparison of one of the components with UV spectral data, density of states (DOS), or with results from theoretical curved-wave multiple scattering cluster calculations (FEFF6 results). The derived Cl L_3 (or L_2) experimental component agrees reasonably well with the calculated DOS and with the FEFF6 results except in the excitonic region. Comparison with the UV spectra reveals a strong similarity between the Cl L_3 (or L_2) component and the UV (Cl M_{23}) spectrum. Through this similarity, we account for peaks in the UV with a one-electron theory, which were previously attributed to two-electron excitations. The excitonic peaks in the UV spectra at the alkali metal edge are similarly analyzed, resulting in assignments different from those previously given in the literature.

I. INTRODUCTION

The x-ray and optical absorption spectra of the alkali halides have been studied extensively utilizing both experimental and theoretical techniques.[1–8] As a result of these and other studies, the electronic and atomic structural (i.e., crystal structures, lattice constants, and Debye temperatures) properties of these materials are rather well understood. Despite this effort, several aspects of the interpretation of near-edge x-ray absorption spectra (NEXAFS) and UV absorption data for the alkali halides are still unclear or controversial. On the other hand, recent theoretical advances, such as the curved-wave multiple scattering cluster theories incorporated in the FEFF6 code,[9] have provided a more quantitative understanding of NEXAFS data and should improve our understanding of the alkali halide spectra. Further, detailed comparisons of the NEXAFS and optical UV absorption data are expected to allow for improved understanding of the UV absorption data.

The Cl L_{23}-edge NEXAFS data for the alkali halides have been reported in several studies.[1–4] Early work compared the experimental data to density-of-states (DOS) results from band structure calculations.[2–5] In general, the comparison with DOS obtained from band structure calculations is not successful due to the uncertainty of the edge position and the exclusion of the core-hole effect. Even when the edge positions are determined with the help of x-ray photoelectron spectroscopy (XPS) and band-gap values, agreement between the calculated DOS and NEXAFS is not good due to the core-exciton peaks,[4] which are not present in the DOS because of exclusion of the core-hole effect. The first 15 eV above the edge in MCl (M=Li–Cs) NEXAFS exhibit excitonic transitions. More recent cluster calculations utilizing multiple scattering theory have been much more successful, particularly when including the effects of the core hole,[5–7] although in some cases still not accounting completely for the excitonic transitions. In addition, a recent model based on the $1/R^2$ correlation suggests that the post-edge features (i.e., 10–50 eV above the edge) may be correlated with interatomic distances and lattice spacings.[8]

In this work, we will be examining the L_{23}-edge NEXAFS data for alkali metal (Na, K, and Rb) chlorides utilizing the recently developed FEFF6 code by Rehr and co-workers.[9] This code incorporates multiple scattering along with the effects of the core hole on a cluster approximating the solid. The experimental Cl L_{23} spectrum is composed of both the L_2 and L_3 components which are separated in energy by only 1.6 eV. On the other hand, theoretical calculations utilizing the FEFF6 code give identical results for both the L_2 and L_3 line shapes. Therefore, in order to compare the theoretical calculations with experimental data, we either have to decompose the experimental L_{23} spectrum into the separated L_2 and L_3 components or reconstruct the L_{23} spectrum from the theoretical L_2 and L_3 components. The former procedure proves to be the more effective method. We present a simple iterative method for accomplishing this task. The isolated L_3 component allows detailed comparison with density-of-states calculations as well as with UV absorption data. Conclusions are reached particularly on the UV data.

II. SEPARATION OF L_{23} COMPONENTS

In order to separate the L_3 component from the L_2 component, it is essential to know the branching ratio $R_{23} = \mu_{L_2}(E)/\mu_{L_3}(E-E_{23})$, where μ is the absorption coefficient, E is the photon energy, and E_{23} is the spin-orbit splitting between the L_3 and L_2 edges. Note that this definition of the branching ratio differs from the usual one, namely, $\mu_{L_3}/(\mu_{L_3}+\mu_{L_2})$. The branching ratio R_{23} for the excitonic levels can be very different from that of the continuum excitations. Thole and van der Laan[10] have shown that two conditions are necessary and sufficient for obtaining the normal statistical ratio [i.e., R_{23}=0.5, since the L_2 ($P_{1/2}$) and L_3 ($P_{3/2}$) states have multiplicities of 2 and 4, respectively]. The

first condition is that the spin-orbit coupling in the initial state must be negligible, and the second that the electrostatic interactions between the core hole and excited electron must be negligible in the final state. All alkali halides have closed-shell electronic structure, and so there is no spin-orbit coupling in the initial state. The electrostatic interaction between the core hole and excited electron is expressed in terms of the Slater integrals F and G, the Coulomb and exchange integrals. Thole and van der Laan[10] found that R_{23} monotonically increases with an increase of these Slater integrals for d^0 compounds (which include alkali halides). For excitations to the continuum, these Slater integrals are small, so that the branching ratio is statistical as demonstrated by XPS data.[11] For excitons, on the other hand, the Slater integrals vary depending on the localization; i.e., R_{23} is large for the localized excitons and small (i.e., around 0.5) for the diffuse excitons, such as Wannier or charge-transfer excitons.

From the opposite perspective, it is possible to determine the localization of the exciton from knowledge of its branching ratio. By a method to be described below, we found R_{23} to be equal to 0.5 for the excitonic peaks in the Cl L_{23} NEXAFS spectrum of KCl. This indicates that these excitons are diffuse. It is well established that these anionic excitons are of the charge transfer type, i.e., localized on the neighboring alkali ions with small electron density around the Cl atom itself.[12] On the other hand, the R_{23} for the excitons at the L_{23} edge on the alkali metal are found to be 1.2 for the excitons. This is consistent with the well-known localized character of these cationic excitons.

The following equation expresses the iterative method we developed to separate the experimental L_{23} spectrum μ_{expt} into the L_2 and L_3 components μ_{i,L_2} and μ_{i,L_3}:

$$\mu_{i+1,L_3}(E)=\{\mu_{i,L_3}(E)+\alpha[\mu_{\text{expt}}(E) - R_{23}\mu_{i,L_3}(E-E_{23})]\}/(1+\alpha). \quad (1)$$

Here i is the number of iteration, α is a convergence control parameter usually chosen to be unity, and as mentioned earlier, E_{23} is the spin-orbit splitting between the L_2 and L_3 edges, which can be obtained from XPS or x-ray fluorescence data. In the case of Cl in MCl, E_{23} is 1.6 eV.[13] This iterative method assumes that $\mu_{L_2}(E)=R_{23}\mu_{L_3}(E-E_{23})$. If the procedure converges, the total absorption $\mu_{L_2}(E)+\mu_{L_3}(E)$ should be very close to the experimental $\mu_{\text{expt}}(E)$ with a unique $\mu_{L_3}(E)$.

As discussed above, $R_{23}(E)$ can be different for the excitonic and continuum energy regions. This requires that the excitonic and continuum energy contributions be isolated so that the iterative procedure can be performed on these isolated contributions with the appropriate R_{23} for each case. Fortunately, we have found for the Cl L_{23} edge that R_{23} is 0.5 for both the excitonic and continuum energy regions, and so we can proceed to use Eq. (1) over the entire spectrum. The results for KCl shown in Fig. 1 were obtained after five iterations, the usual number required for convergence.

Previously Sagawa *et al.*[1] used a somewhat different technique to separate the L_3 and L_2 components. They also assumed $R_{23}=0.5$ and $E_{23}=1.6$ eV. Since the experimental spectrum less than 1.6 eV above the L_3 edge (i.e., below the

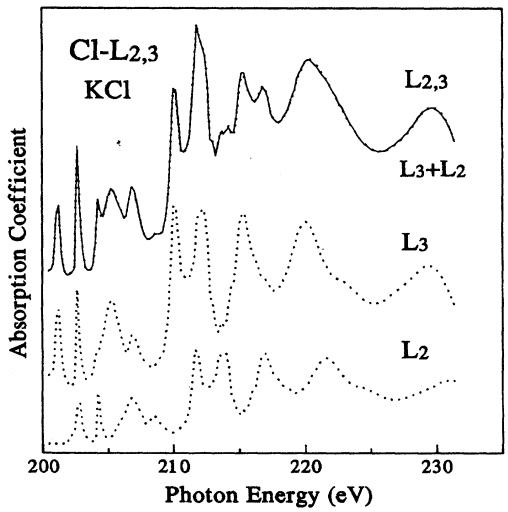

FIG. 1. Comparison of the theoretical total absorption L_3+L_2 with the experimental L_{23} Cl NEXAFS data for KCl (Ref. 3) and the separated components where $\mu_{L_2}(E)=R_{23}\mu_{L_3}(E-E_{23})$.

L_2 edge) is due wholly to the L_3 component, they subtracted half of it from the next 1.6-eV interval, i.e., between 1.6 and 3.2 eV. This interval after subtraction is then equal to the L_3 component in the same interval range. This process continues until the entire spectrum is separated into the L_2 and L_3 components. This method relies greatly on the accuracy of the first 1.6-eV energy interval. Any error in this region will be carried along the entire energy range. This method also fundamentally requires that R_{23} be the same for the excitonic and continuum energy regions, which generally is not the case as discussed above, although it is true for the Cl L_{23} NEXAFS discussed here. The experimental spectrum Sagawa *et al.*[1] used for KCl had much lower resolution than the one we use (0.3 eV) here.[3]

Our iterative method fundamentally assumes that the L_2 and L_3 contributions have identical shapes, i.e., $\mu_{L_2}(E)=R_{23}\mu_{L_3}(E-E_{23})$. This is not always the case, particularly in the excitonic region. For example, the K^+ (L_{23}) NEXAFS spectrum for KCl in Fig. 7 (to be discussed later) reveals a slightly different width for the L_2 and L_3 contributions. The different widths arise because of the different lifetimes of the core hole. Thus some care must be exercised for general use of this method.

Equation (1) could in principle be used to obtain R_{23}. To illustrate this, we show results in Fig. 2 for three different chosen values of R_{23}. The 0.5 value more cleanly divides the individual peaks in the excitonic region into the L_2 and L_3 contributions, revealing that this is the preferred value for R_{23}, but this division is not definite since the variation with R_{23} is not that dramatic. A much better method for determining R_{23}, and the one utilized in this work is to isolate the excitonic part of the spectrum and individually fit Gaussian or Lorentzian line shapes to the peaks to obtain their relative intensities. This procedure takes into account the different widths and thereby accurately gives R_{23}. Thus Eq. (1) is best utilized to separate only the continuum part of the spectrum into the L_2 and L_3 contributions using the statistical

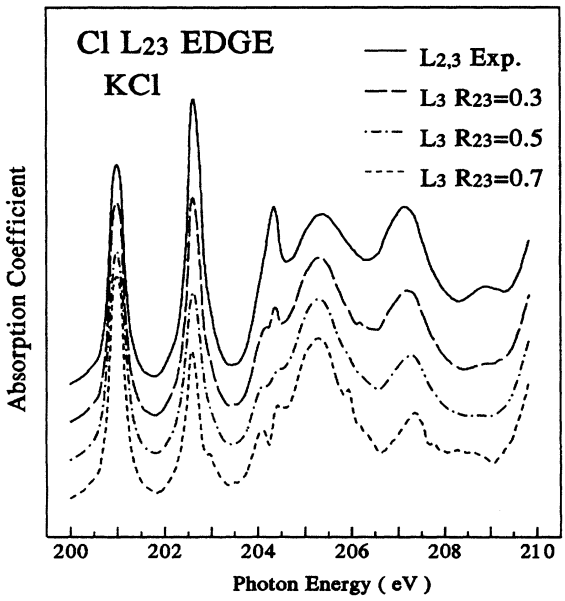

FIG. 2. Comparison of the experimental Cl L_{23} NEXAFS line shape ("excitonic region") with the L_3 component obtained from Eq. (1) assuming different branching ratios (R_{23}).

$R_{23}=0.5$; separation of the excitonic region into the L_2 and L_3 contributions is generally best accomplished by peak fitting as described immediately above.

III. COMPARISON OF EXPERIMENTAL AND THEORETICAL Cl L_{23} EDGE RESULTS

We used the FEFF6 code recently developed by Rehr and co-workers[9] to calculate the near-edge structure of the Cl L_2 or L_3 edges for NaCl, KCl, and RbCl. Curved-wave multiple scattering calculations are performed on large clusters approximating the solid. The clusters we use have fcc structures and contain 10 shells with a total of 154 atoms. The input parameters to the code were varied to give optimal agreement with experimental data. The longest path lengths "$R_{\max}$ were set at around 11 Å (we found that increasing $R_{\max}$ beyond this value reduced some of the multiple scattering paths). The path filter parameter CRITERIA was set to the minimum so that we could maximize the number of paths possible with the code. The ground-state exchange potential was utilized with a constant imaginary part $E_i=0.3$ eV, which was chosen such that the instrumental broadening [0.3 eV (Ref. 4)] can be accounted for. Since the Debye-Waller factor does not have a significant effect on the amplitudes at the sample temperature of 77 K,[3] vibrational effects were ignored. Figure 3 compares theoretical L_3 results with the "experimental" L_3 component obtained using Eq. (1).

Figure 4 shows a more detailed comparison of the separated L_3 component for KCl with FEFF6 results and the Cl d-projected density of states (PDOS) for KCl. The PDOS was calculated by Gegusin *et al.*[14] using the augmented-plane-wave (APW) method. Both calculations fail to reproduce the excitonic peaks E_1 and E_2, as expected. However, both theoretical results agree somewhat with the experimental data at higher energies, at least in reproducing all resonant features R_1-R_8 (except R_7 by the FEFF6 calculations). Note that the DOS result, unlike the FEFF6 result, does not include the dipole matrix elements. Therefore, the relative peak heights could be different between the two results because of the energy variation in the matrix elements. Based on the fact that multiple-electron excitations generally produce identifiable features in the spectrum and the one-electron results

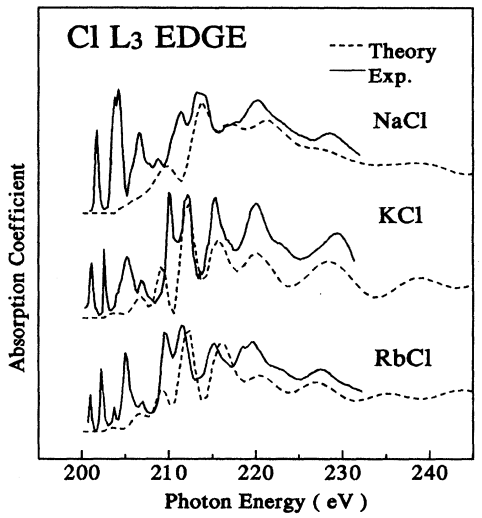

FIG. 3. Comparison of the "experimental" L_3 component obtained from Eq. (1) with FEFF6 results. Experimental data from Watanabe (Ref. 3) were used to obtain the L_3 component. The theoretical results have been optimally aligned with the experimental data.

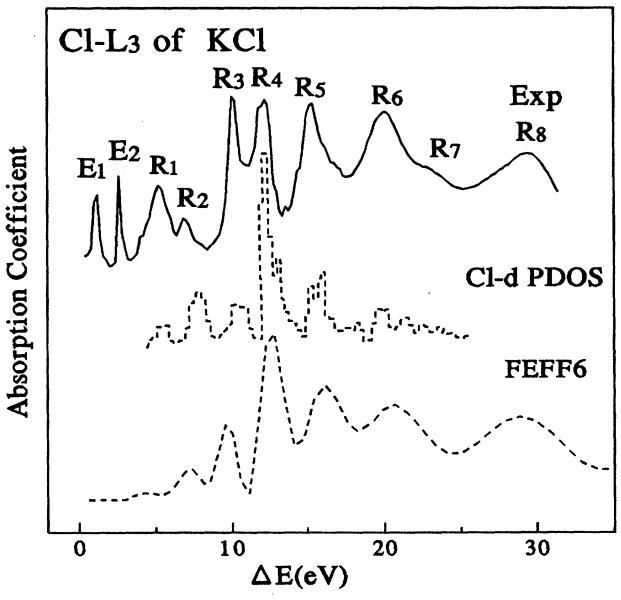

FIG. 4. Comparison of the L_3 component for KCl from Fig. 1 with Cl d PDOS (Ref. 14) and FEFF6 theoretical results. The theoretical results have been optimally aligned with the experimental data.

reproduce all of the visible features, we conclude that multiple-electron contributions are small here. However, we cannot rule out the presence of much smaller multiple-electron features, such as those which become visible in the very-high-resolution data available for the rare gas solids.[15]

To weigh possible reasons for the disagreement found between FEFF6 results and experiment for energies above the excitonic region, it is helpful to compare the quality of the agreement found here for the L_3 level with the agreement found elsewhere for the K-level NEXAFS data. Both the alkali halides and the solid rare gases, assuming total charge transfer, have rare-gas closed-shell electronic configurations. Agreement for the rare-gas solids is nearly quantitative, with only the excitonic features and the very small sharp multiple-electron peaks not reproduced by the FEFF6 results.[17] The agreement for the K-level alkali halide data[17] is also good, at least much better than for the L_3 level shown in Figs. 3 and 4, although not as good as for the rare-gas solids. Recently, K-level FEFF5 (Ref. 7) results have been reported for the alkali halides, which show significantly worse agreement with experiment than does the FEFF6 results.[17]

It is well known that in the alkali halides MX, a large charge transfer occurs between the metal and halide; i.e., ions exist with the nominal charge M^+ and X^-. However, only positive ions can be assigned in the code; negative charges on the halide atoms cannot be assigned. We assumed neutral atoms instead of ions for the calculations. It has been asserted that an all-neutral-atom calculation should not produce a significant error, since any transferred charge to the anion which may actually occur exists in a diffuse orbital which will not significantly scatter 10–50 eV electrons anyway.[16] Nevertheless, since the agreement with experiment for the alkali halides is not as good as for the condensed rare gases,[17] this may result from the charge transfer not included in the calculations.

The dipole selection rule $\Delta l=\pm 1$ indicates that the L_{23} edge should exhibit contributions from both the s and d waves. The FEFF6 code, however, allows only one final-state angular momentum, and this is always the larger one (i.e., the d wave in this case). The s wave is believed to contribute at lower energies. This may account for some of the discrepancy between theory and experiment in this range[18] and also may account for the larger disagreement between theory and experiment for the L_3-level vs the K-level data. In the latter, only the p wave can contribute. However, the d orbitals reflected in the L_3 edge are expected to have a larger radius and hence undergo more covalent interaction with its neighbors in the lattice than the p orbitals reflected in the K edge. Therefore, the decreased quality of the agreement for the L_3 NEXAFS may also reflect increased breakdown in the scattered-wave muffin-tin approximation used in the FFEF6 calculations.

The FEFF6 code gives the exact same $\mu(E)$ for the L_2 and L_3 components. It is easy to construct the theoretical μ for the L_{23} edge with the known R_{23} and ΔE_{23}. In fact, we have constructed the theoretical $\mu_{L_{23}}$ spectra and directly compared it with the experimental data without decomposition. Differences between the theory and experimental results are so large that it is difficult to make a correlation. It is essential therefore to separate the experimental L_2 and L_3 components for a meaningful comparison between theory and experiment. Furthermore, this separation allows direct comparison with the UV absorption data, as demonstrated below.

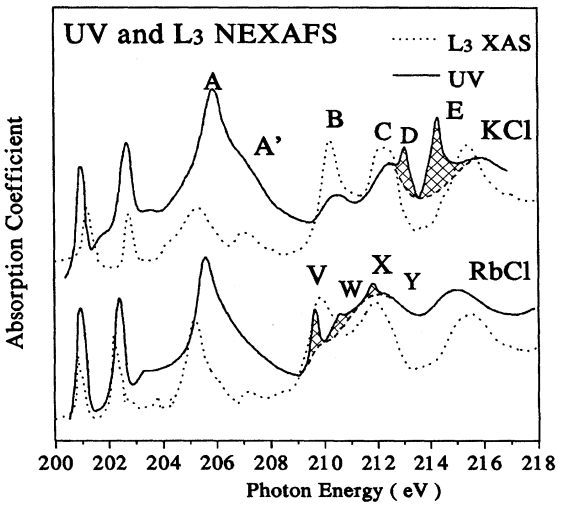

FIG. 5. Comparison of the "experimental" L_3 component for KCl and RbCl (see Fig. 3) with UV experimental data obtained from Watanabe *et al.* (Ref. 19). The estimated contributions arising from the alkali metal excitonic excitations are shaded. The energy scale is that for the experimental NEXAFS data, and the UV spectra have been optimally shifted upward by 192.8 eV for KCl and 193.5 eV for RbCl. This is reasonably consistent with the energy separation between the $2p$ and $3p$ atomic shells in Cl^- (i.e., $\Delta E=201-9$ eV) (Refs. 27, 28).

IV. COMPARISON OF Cl(L_3) NEXAFS COMPONENT WITH UV SPECTRA

The UV spectra[19] in the alkali chlorides mainly arise from excitations out of the Cl $3p$ valence band. Since the Cl L_{23} edge arises from transitions out of the Cl $2p$ core level (i.e., orbitals of the same symmetry), it is natural to compare the two spectra. Furthermore, since the spin-orbit splitting of the $3p^5$ state is negligible and the width of the Cl $3p$ valence band is narrow enough to avoid having to consider the joint density of states, the UV spectra can be directly compared with the L_3 component. However, in the UV spectra, peaks resulting from transitions out of the metal valence p orbital can also appear. The shaded peaks D and E in KCl and V, W, X, and Y in RbCl (Fig. 5) have been previously identified as such excitonic transitions due to excitation out of the metal valence orbitals.[19,20] We shall discuss these peaks below. If we disregard these peaks, we see almost a one-to-one correspondence between peak energies in the Cl L_3 component and the UV data (Fig. 5). The relative peak heights are, however, substantially different especially for the relative intensity below and above 210 eV, because of the different energy dependence in their matrix elements.

The shoulder A' in the UV spectrum for KCl (Fig. 5) has attracted the attention of several workers. This shoulder has been attributed to a plasmon or to two-electron excitations.[21] However, the separated Cl L_3 spectrum shows a corresponding feature R_2 (see Figs. 4 and 5) and this R_2 feature is reproduced by both the FEFF6 and PDOS calculations (Fig.

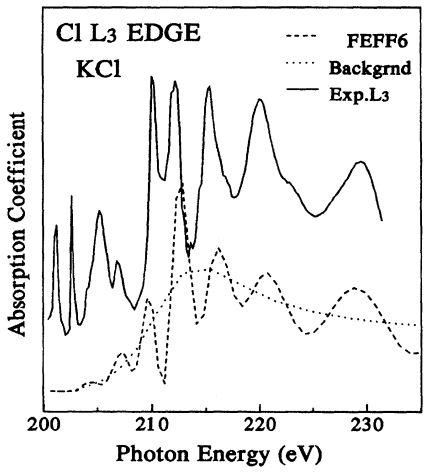

FIG. 6. Atomic background contribution to the theoretical FEFF6 results for the Cl L_3 of KCl are shown along with the total (i.e., atomic background plus scattering contribution) and the "experimental" L_3 component (Fig. 1).

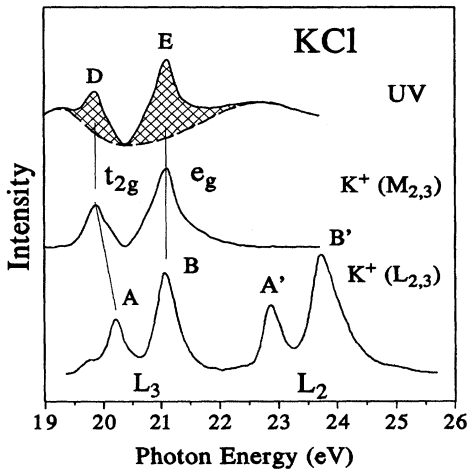

FIG. 7. Comparison of the experimental KCl UV and L_{23} spectra in the K^+ excitonic region. The energy scale indicated is that for the UV spectrum: the L_{23} spectrum has been shifted by 275 eV for best peak alignment, consistent with the energy separation of the $3p$ and $2p$ atomic orbitals in K^+ ($\Delta E=296-21$ eV) (Refs. 27, 28). The spectrum labeled K^+ (M_{23}) has the Cl (M_{23}) contribution subtracted (i.e., replots the shaded region).

4), both of which account only for one-electron excitations. Therefore, we suggest that the R_2 feature in the Cl L_3 NEXAFS and the A' shoulder in the UV spectrum for KCl arise from a one-electron transition.

There is an apparent intensity enhancement of the background around 210 eV in the Cl L_3 component for both KCl and RbCl (see Figs. 1 and 5), which appears to be absent or at least much diminished in the UV data. Why should the background suddenly increase almost 8 eV above the L_3 edge at 200.9 eV? Vedrinskii *et al.*[5] concluded that the apparent background enhancement originates from the atomiclike contribution $\mu_0(E)$. Watanabe[3] also attributed the background to the atomiclike contribution and further suggested that the delayed onset arises because of the nature of the $p\rightarrow d$ transition, where the large angular momentum barrier pushes the d DOS well above the edge. Comparison of the "experimental" L_3 component with the calculated NEXAFS line shape (Fig. 6), now showing the atomic contribution $\mu_0(E)$ and total $\mu(E)$, confirms that the enhancement in the L_3 NEXAFS is indeed due to the atomiclike background contribution.

The absence of this comparable background enhancement in the UV data apparently arises from the relative weighting of the excitonic and continuum contributions. Comparison of the M_{23}, L_{23}, and K absorption spectra suggests that the intensity of the excitonic contributions increase with respect to the continuum contributions as the binding energy of the initial hole state decreases. This may arise from the relative magnitude of the dipole transition matrix elements. In any event, the large relative increase of the excitonic contribution in the UV spectra nearly dwarfs the atomic continuum contribution, so that little enhancement in the background is now evident.

V. COMPARISON OF METAL-EDGE NEXAFS WITH UV SPECTRA

Peaks D and E (for KCl) and V, W, X, and Y (for RbCl) in the UV spectra (Fig. 5) have been identified, respectively, as the metal K^+ (M_{23}) and Rb^+ (N_{23}) transitions, rather than the Cl^- (M_{23}) transitions.[19,20] These identifications are confirmed by a study on solid solutions of KCl and RbCl.[19] Comparison of the UV and the Cl (L_3) spectra (Fig. 5) also supports these identifications. Further, specific electronic transitions have been attributed to those peaks: i.e., the K^+ ($3p\rightarrow 4s$) and K^+ ($3p\rightarrow 3d$) transitions to peaks D and E, respectively;[22] the Rb^+ ($4p\rightarrow 5s$) and Rb^+ ($4p\rightarrow 4d$) transitions to the four peaks V, W, X, and Y.[23] Below we shall propose alternative electronic transitions by comparing the UV spectra with the corresponding metal-edge NEXAFS spectra.

Figure 7 shows the K^+ (L_{23})-edge NEXAFS spectrum of KCl measured by Sette *et al.*[24] The origin of the four peaks A,B,A',B' has been extensively studied recently[25] and now can be considered well established. That is, all four peaks arise from the K^+ ($2p\rightarrow 3d$) transition. [We emphasize that de Groot *et al.*[25] explained every detail of the spectrum including the weak feature at the threshold without invoking the K^+ ($2p\rightarrow 4s$) transitions.] The (A,B) and (A',B') pairs are, respectively, the $2p_{3/2}(L_3)$ and $2p_{1/2}(L_2)$ components of the spin-orbit-split K^+ ($2p^5$) hole. The spin-orbit splitting of the K^+ ($2p^5$) hole is known to be around 2.8 eV from XPS data.[11] The A and B (A' and B') peaks arise from the crystal-field splitting of the $3d$ orbital into the $t_{2g}(A,A')$ and $e_g(B,B')$ orbitals in the octahedral crystal field. Since the e_g orbital is more antibonding than the t_{2g} orbital, the linewidths of the $e_g(B,B')$ lines are wider than those of the $t_{2g}(A,A')$ peaks as seen in Fig. 7. Our interpretation of the D and E peaks in the UV spectrum for KCl is based on these assignments of the A, B, A', and B' peaks in the K^+ (L_{23}) NEXAFS spectrum.

We now compare in Fig. 7 the K^+ ($2p\rightarrow 3d$) peaks in the L_{23} spectra with the K^+ ($3p\rightarrow 3d$) peaks in the UV. The K^+ (M_{23}) spectrum in Fig. 7 is obtained by removing the Cl^-

(M_{23}) contributions from the UV spectrum. In contrast to the K^+ ($2p \rightarrow 3d$) transitions, the K^+ ($3p \rightarrow 3d$) transitions give rise to only two peaks, because the spin-orbit splitting of the K^+ ($3p^5$) hole is negligibly small; i.e., the K^+ (M_3) and K^+ (M_2) spectra coincide with each other. The relative intensities, the relative widths, and the ordering of the t_{2g} and e_g peaks for the K^+ ($2p \rightarrow 3d$) and K^+ ($3p \rightarrow 3d$) transitions are expected to be the same or similar. The absence of the K^+ ($2p \rightarrow 4s$) transitions in the K^+ (L_{23}) indicates that the K^+ ($3p \rightarrow 4s$) transitions should also be absent in the K^+ (M_{23}) spectrum. (The $4s$ orbital is Rydberg like in nature and very diffuse; the disappearance of diffuse Rydberg orbitals in solids has been demonstrated in many cases previously.) Based on the above, we attribute the t_{2g} and e_g states of the K^+ ($3p \rightarrow 3d$) transitions to the D and E peaks.

We believe that the Rb^+ ($4p \rightarrow 5s$) transitions also do not contribute significantly to the Rb^+ (N_{23}) spectrum, contrary to a previous assignment.[23] We propose that all four features (V,W,X,Y) in the Rb^+ (N_{23}) spectrum arise from the Rb^+ ($4p \rightarrow 4d$) transitions, which give four peaks due to a sizable spin-orbit splitting ($\approx$0.9 eV) of the Rb^+ ($4p^5$) valence hole along with the crystal-field splitting. The irregular intensities and spacing of the V, W, X, and Y features can be attributed to the similar magnitudes of the spin-orbit splitting ($\approx$0.9 eV) and crystal-field splitting ($<$1.4 eV). This makes the second and third states have similar energies and hence have a strong interaction.

Figure 7 shows that the crystal-field splitting of the $d(t_{2g})$ and $d(e_g)$ orbitals increases from 0.9 eV for K^+ ($2p \rightarrow 3d$) to 1.5 eV for K^+ ($3p \rightarrow 3d$). This increase arises because the size of the $3d$ orbital increases from the K^+ ($2p \rightarrow 3d$) final state to the K^+ ($3p \rightarrow 3d$) final state. We can estimate the size of the $3d$ orbitals for these cases by calculating $\langle r \rangle_{3d}$ and $\langle r^2 \rangle_{3d}$ expectation values with Slater orbitals, $r^{n-1} \exp[-(Z-s)r/n]$, where the shielding parameter s is determined according to Burns' rules.[26] The resultant $\langle r \rangle_{3d}$ and $\langle r^2 \rangle_{3d}$ are 1.01 Å and 1.17 Å^2 for K^+ ($2p \rightarrow 3d$) and 1.11 Å and 1.41 Å^2 for K^+ ($3p \rightarrow 3d$). As the size of the $3d$ orbital increases, the overlap between the $3d$ orbitals and the ligand orbitals increases and therefore the crystal-field splitting increases, as observed in Fig. 7. The overlap integral is a very sensitive function of the $3d$ orbital size and can account for the observed large variation in the crystal-field splittings.

VI. SUMMARY

We have developed an effective iterative decomposition procedure for separating the L_{23} line shape into the L_2 and L_3 components. This allows a direct comparison of one of the components with UV spectral data, with DOS results, or with FEFF6 results. Comparison of the L_3 component with DOS calculations and with the FEFF6 calculations reveals reasonable agreement, except in the excitonic region, and poorer agreement than those found previously for the K-level data in the alkali halides and solid rare gases. Possible reasons for this have been given.

Comparison with the UV spectra reveals a strong similarity between the Cl L_3 (L_2) component and UV (Cl M_{23}) spectrum. Through this comparison, we account for peaks with a one-electron theory, some of which were previously attributed to two-electron excitations. We also assign the excitonic peaks in the UV spectra at the alkali metal edge. These assignments indicate that all of the peaks arise from the crystal-field and spin-orbit splitting in the final state of the $p \rightarrow d$ excitations in both KCl and RbCl. Evidence indicates that the $p \rightarrow s$ excitations are negligible in contrast to that suggested previously.

Finally, for the alkali halides, we found that there is better agreement between the experimental NEXAFS and UV data than between the FEFF6 results and the experimental NEXAFS data. This suggests that the FEFF6 code, which was initially designed to interpret NEXAFS data, could also be used to interpret UV data, particularly in those cases where conditions exist, as in the alkali halides, where the UV data is dominated by excitation out of a single closed shell. Its validity for other UV data remains to be tested.

Support from the Office of Naval Research was gratefully acknowledged.

[1] T. Sagawa, Y. Iguchi, M. Sasanuma, T. Nasu, S. Yamaguchi, S. Fujiwara, M. Nakamura, A. Ejiri, T. Masuoka, T. Sasaki, T. Oshio, J. Phys. Soc. Jpn. **21**, 2587 (1966); O. Aita, I. Nagakura, and T. Sagawa, *ibid.* **30**, 1414 (1971).

[2] F. C. Brown, C. Gahwiller, H. Fujita, A. B. Kunz, W. Scheifley, and N. Carrera, Phys. Rev. B **2**, 2126 (1970).

[3] M. Watanabe, J. Phys. Soc. Jpn. **34**, 755 (1973).

[4] S. T. Pantelides and F. C. Brown, Phys. Rev. Lett. **33**, 298 (1974); S. T. Pantelides, Phys. Rev. B **11**, 2391 (1975).

[5] R. V. Vedrinskii, L. A. Bugaev, I. I. Gegusin, V. L. Kraizman, A. A. Novakovich, S. A. Rosandeev, R. E. Ruus, A. A. Maiste, and M. A. Elango, Solid State Commun. **55**, 1401 (1982); Phys. Status Solidi **133**, 195 (1986); **132**, 459 (1985); **134**, 641 (1986); J. Phys. (Paris) Colloq. **47**, C8-97 (1986); **47**, C8-101 (1986).

[6] A. V. Soldatov, T. S. Ivanchenko, I. E. Stekhin, and A. Bianconi, J. Phys. Condens. Matter **5**, 7521 (1993).

[7] E. Hudson, E. Moler, Y. Zheng, S. Kellar, P. Heimann, Z. Hussain, and D. A. Shirley, Phys. Rev. B **49**, 3701 (1994).

[8] M. Kasrai, M. E. Fleet, G. M. Bancroft, K. H. Tan, and J. M. Chen, Phys. Rev. B **43**, 1763 (1991).

[9] J. Mustre de Leon, J. J. Rehr, S. I. Zabinsky, and R. C. Albers, Phys. Rev. B **44**, 4146 (1991); J. J. Rehr, Jpn. J. Appl. Phys. Suppl. **32**, 8 (1993).

[10] B. T. Thole and G. van der Laan, Phys. Rev. B **38**, 3158 (1988).

[11] P. H. Citrin, P. Eisenberger, and D. R. Hamann, Phys. Rev. Lett. **33**, 965 (1974).

[12] K. Teegarden and G. Baldini, Phys. Rev. **155**, 896 (1967).

[13] C. Sugiura, J. Phys. Soc. Jpn. **62**, 585 (1993).

[14] I. I. Gegusin, V. N. Datsyuk, and R. V. Vedrinskii, Phys. Status Solidi B **109**, 563 (1982).

[15] A. Hiraya, K. Fukui, P. K. Tseng, T. Murata, and M. Watanabe, J. Phys. Soc. Jpn. **60**, 1824 (1991).

[16] J. J. Rehr (private communication).

[17] D. E. Ramaker, H. Sambe, X. Qian, and W. E. O'Grady, Physica

B **208/209**, 49 (1995).
[18] T. M. Zimkina and A. P. Lukirskii, Sov. Phys. Solid State **7**, 1175 (1965).
[19] M. Watanabe, Y. Nakamura, Y. Nakai, and T. Murata, J. Phys. Soc. Jpn. **26**, 1014 (1969).
[20] H. Saito, S. Saito, R. Onaka, and B. Ikeo, J. Phys. Soc. Jpn. **24**, 1095 (1968); R. Onaka, H. Saito, and S. Saito (unpublished).
[21] J. T. Devreese, A. B. Kunz, and T. C. Collins, Solid State Commun. **11**, 673 (1972).
[22] M. Shibowski, G. Sprussel, and V. Saile, Appl. Opt. **19**, 3978 (1980).
[23] C. Satoko and S. Sugano, J. Phys. Soc. Jpn. **34**, 701 (1973).
[24] F. Sette, B. Sinkovic, Y. J. Ma, and C. T. Chen, Phys. Rev. B **39**, 11 125 (1989).
[25] F. M. F. de Groot, J. C. Fuggle, B. T. Thole, and G. A. Sawatzky, Phys. Rev. B **41**, 928 (1990).
[26] G. Burns, J. Chem. Phys. **41**, 1521 (1964).
[27] R. T. Poole, J. G. Jenkin, J. Liesegang, and R. C. G. Leckey, Phys. Rev. B **11**, 5179 (1975).
[28] *Topics in Applied Physics*, edited by M. Cardona and L. Ley (Springer-Verlag, Berlin, 1978), Vol. 26, p. 266.